Photoelectrochemical and Quenching Studies of Tris(2,2′-bipyridine)ruthenium(II) bound to Nafion- and Clay-coated Electrodes

K. Vengatajalabathy Gobi and Ramasamy Ramaraj*
School of Chemistry, Madurai Kamaraj University, Madurai 625 021, Tamilnadu, India

The photosensitizer $[Ru(bipy)_3]^{2+}$ (bipy = 2,2′-bipyridine) was adsorbed on Nafion(nf)- and bentonite clay(bt)-coated electrodes. Photoelectrochemical cells were constructed using Pt–nf–$[Ru(bipy)_3]^{2+}$ and Pt–bt–$[Ru(bipy)_3]^{2+}$ electrodes with cobalt(III) complexes and Fe^{3+} ion as electron relays. At appropriate applied potentials, anodic and cathodic photocurrents were induced when the electrodes were irradiated with visible light in solutions containing a mixture of a cobalt(III) complex and $HClO_4$. The photoresponse could be switched between anodic and cathodic by controlling the applied electrode potential. The origin of the photocurrent is explained by an oxidative quenching by the cobalt(III) complex of the photoexcited $^*[Ru(bipy)_3]^{2+}$ complex confined at the electrode, followed by electrochemical reduction or oxidation of the resulting $[Ru(bipy)_3]^{3+}$ and cobalt(II) complex respectively. The quenching rate constants, k_q, for the reaction of $^*[Ru(bipy)_3]^{2+}$ with three different cobalt(III) complexes and Fe^{3+} ion were determined by photoelectrochemical methods.

In recent years much attention has been paid to the investigation of chemically modified electrodes.[1–6] One of the reasons given is the desire to obtain a photocurrent.[1,2,7–10] Photoresponsive electrodes are attracting much attention in the field of light sensors as well as in solar-energy conversion devices.[11,12] The photosensitizer tris(2,2′-bipyridine)ruthenium(II), $[Ru(bipy)_3]^{2+}$, strongly absorbs visible light and produces highly oxidizing and reducing agents $[Ru(bipy)_3]^{3+}$ and $[Ru(bipy)_3]^{+}$ *via* an oxidative and a reductive quenching reaction with suitable quenchers.[1,2,7,12–17] Photochemical processes occurring in a photoredox system will often depend not only on the reagent–quencher pair but also on their immediate environment. When components of a photoredox system are bound to chemically modified electrodes the bimolecular quenching reaction can be accelerated.[18] Nafion and clays have already been used as coating materials to prepare modified electrodes.[19–22] Nafion provides a unique solid matrix containing a fluorocarbon backbone with pendant chains terminated with sulfonate head groups which are responsible for its ion-exchange and swelling properties.[23,24] Yeager and Steck[25] proposed a three-phase structure, *i.e.* a hydrophobic fluorocarbon phase, hydrophilic sulfonate-ion cluster region and an interfacial region between these two. The unique multidomain structure of the Nafion polymer membrane, which provides binding sites for both hydrophobic and hydrophilic molecules, made it the most attractive material for electrode modification.[26,27] Clay minerals are hydrous layer silicates of the so-called phyllosilicate family, in which the extremely stable SiO_4 tetrahedral structural unit has been polymerized to form two-dimensional sheets.[28,29] Owing to isomorphous substitution of one atom with another of lower valency in the clay matrix, the clay possesses a net negative charge which leads to significant cation-exchange capacity.[30,31] Therefore the photoredox molecules of interest $\{[Ru(bipy)_3]^{2+}$, cobalt(III) complex, *etc.*$\}$ can be adsorbed easily at Nafion- and clay-modified electrodes.

Rong *et al.*,[2] Kaneko and Yamada,[12] and Kaneko[32] reported the generation of anodic and cathodic photocurrents at bilayer coated electrodes with different applied potentials. Herein we report the generation of anodic and cathodic photocurrents at Nafion- and clay-coated electrodes containing $[Ru(bipy)_3]^{2+}$ dipped in a solution of cobalt(III) complex or Fe^{3+} ion. The rate constant for the oxidative quenching reaction of $^*[Ru(bipy)_3]^{2+}$ adsorbed onto Nafion- or bentonite clay-coated electrodes with different cobalt(III) complexes as quenchers were also determined using a photoelectrochemical cell.

Experimental

Materials.—Nafion 117 (1100 EW) (Aldrich, 5% solution) was diluted to 1% solution using methanol before use. Bentonite clay (Aldrich) was purified by sedimentation, centrifugation and drying in air. The dried clay was resuspended in distilled water (0.1 g per 100 cm^3) and stirred for 6 h before coating on the electrode. The complex $[Ru(bipy)_3]Cl_2$ was prepared according to the literature procedure,[33] as were $[Co(cyclam)(H_2O)_2][ClO_4]_3$[34,35] (cyclam = 1,4,8,11-tetraazacyclotetradecane), $[Co(hmtd)(H_2O)_2][ClO_4]_3$[36,37] (hmtd = 5,5,7,12,12,14-hexamethyl-1,4,8,11-tetraazacyclotetradecane) and $[Co(hmtd)(H_2O)(NO_2)][ClO_4]_2$.[37] The H^+- and Na^+-exchanged bentonite clays (H^+-bt and Na^+-bt) were prepared using described procedures.[38,39] Ammonium iron(III) sulfate, triethanolamine and other chemicals were of analytical grade used without further purification.

Apparatus and Methods.—For electrochemical and photoelectrochemical measurements, a EG & G PAR model 273A potentiostat/galvanostat equipped with a RE 0151 recorder was used. A three-electrode cell [1 cm^2 platinum plates as working and counter electrodes and a saturated calomel electrode (SCE) as reference electrode] was used to record the cyclic voltammograms and photocurrents. A 150 W xenon lamp (Photon Technology International) was used as light source with water cell and Pyrex-glass filters.

The Nafion- or bentonite clay-coated platinum electrode (Pt–nf or Pt–bt) was prepared by casting a known amount of Nafion (nf) or bentonite clay (bt) solution onto a platinum plate (1 cm^2) and dried at room temperature. The thicknesses of the Nafion and bentonite clay films were estimated to be 1 and 1.19 μm respectively, according to the literature procedures.[11,40] The coated electrodes were dipped into an aqueous solution (5 cm^3) containing 10 mmol dm^{-3} $[Ru(bipy)_3]^{2+}$ for 15–30 min, washed with distilled water and used for experiments after 12–24 h {represented as Pt–nf–$[Ru(bipy)_3]^{2+}$ and Pt–bt–[Ru

$(bipy)_3]^{2+}\}$. The amount of $[Ru(bipy)_3]^{2+}$ adsorbed was determined by spectrophotometry (λ_{max} = 452 nm, ε_{452} = 14 600 dm^3 mol^{-1} cm^{-1}). Electrode potentials were measured and are quoted with respect to a SCE. After replacing the dissolved oxygen gas in the experimental solution with purified nitrogen gas, all electrochemical and photoelectrochemical measurements were carried out at room temperature.

Results and Discussion

The cyclic voltammograms recorded for the $[Ru(bipy)_3]^{2+/3+}$ couple using Pt–nf–$[Ru(bipy)_3]^{2+}$ and Pt–H^+-bt–$[Ru(bipy)_3]^{2+}$ electrodes in a solution containing 0.1 mol dm^{-3} $HClO_4$ are shown in Fig. 1. For both $[Ru(bipy)_3]^{2+/3+}$ and $Fe^{3+/2+}$ redox couples the $E_{\frac{1}{2}}$ values are more negative at the Pt–nf–$[Ru(bipy)_3]^{2+}$ electrode than those at Pt–H^+-bt–$[Ru(bipy)_3]^{2+}$:1.005 and 0.410 and 1.075 and 0.475 V *vs.* SCE, respectively. Liu and Anson[41] observed such shifts in the redox potentials of different couples, *e.g.* $[Ru(NH_3)_6]^{3+/2+}$ and $[Ru(bipy)_3]^{2+/3+}$ at Nafion- and clay-coated electrodes. They, Lieber *et al.*,[42] Naegeli *et al.*,[43] and Gomez and Kaifer[44] explained the negative shift in redox potential as indicating a more favourable partition coefficient and stabilization of the more highly positively charged member of the redox pair in Nafion film. This is expected from stronger electrostatic interactions with the negatively charged sulfonic groups of the film. Conversely, the positive shift in redox potential at clay-coated electrodes shows that the less charged member of each redox couple is more stabilized and tightly bound to the clay coating. For both electrodes the plot of peak current (i_p) *vs.* square root of the scan rate, $\bar{v}$, is linear as shown in Fig. 1 (inset). This clearly demonstrates that the electron-transfer process within the film is diffusion controlled and very similar to that occurring in solution.[45]

The cyclic voltammograms obtained for 0.15 mmol dm^{-3} $[Co(cyclam)(H_2O)_2]^{3+}$ at Pt–nf, Pt–nf–$[Ru(bipy)_3]^{2+}$, Pt–H^+-bt and Pt–H^+-bt–$[Ru(bipy)_3]^{2+}$ electrodes in a solution containing 0.1 mol dm^{-3} $HClO_4$ are shown in Fig. 2. The $E_{\frac{1}{2}}$ values are more negative at Nafion- than at clay-coated electrodes. At all four electrodes the plot of peak current *vs.* $v^{\frac{1}{2}}$ is linear as shown in Fig. 2 (inset). However, at the Pt–H^+-bt and Pt–H^+-bt–$[Ru(bipy)_3]^{2+}$ electrodes some deviation from linearity was observed at higher scan rates (> 50 mV s^{-1}), Fig. 2 (*c*) and (*d*) (inset). Thus the charge-transfer process occurring at the Nafion- and clay-coated electrodes is diffusion controlled.[45]

The photoresponses observed for Pt–nf–$[Ru(bipy)_3]^{2+}$ and Pt–H^+-bt–$[Ru(bipy)_3]^{2+}$ electrodes dipped in an aqueous solution containing 0.15 mmol dm^{-3} $[Co(cyclam)(H_2O)_2]^{3+}$ and 0.1 mol dm^{-3} $HClO_4$ upon irradiation with visible light at applied potentials of 0 and 1.3 V *vs.* SCE are shown in Fig. 3. Cathodic or anodic photocurrents were obtained depending upon the applied potential. At both electrodes, cathodic photocurrents were induced at the bias potential of 0 V *vs.* SCE, while anodic photocurrents were induced at 1.3 V (Fig. 3). The photocurrent rapidly builds to a maximum and continues at a near steady state until the light is turned off. It takes *ca.* 20 s for the photocurrent to become stationary. This phenomenon is typical of a photogalvanic cell. At the two electrodes, cathodic photocurrents of 17 and 24 µA cm^{-2} respectively were observed at the applied potential of 0 V *vs.* SCE under the above conditions, where the amounts of $[Ru(bipy)_3]^{2+}$ adsorbed were 4.05×10^{-8} and 3.75×10^{-8} mol cm^{-2}, respectively. The concentrations of the $[Ru(bipy)_3]^{2+}$ complex at the electrodes were calculated to be 0.41 and 0.32 mol dm^{-3}, respectively. In the absence of $[Ru(bipy)_3]^{2+}$ at the coated electrode or $[Co(cyclam)(H_2O)_2]^{3+}$ in solution a photoresponse was not observed. Cathodic and anodic photocurrents were also observed with Pt–Na^+-bt–$[Ru(bipy)_3]^{2+}$ electrodes at applied electrode potentials of 0 and 1.3 V *vs.* SCE. The cathodic and anodic photocurrents generated with Pt–nf–$[Ru(bipy)_3]^{2+}$ and Pt–H^+-bt–$[Ru(bipy)_3]^{2+}$ electrodes at applied potentials of 0 and 1.3 V *vs.* SCE using four different quenchers are shown in Table 1. At Nafion-coated electrodes the magnitude of the anodic photocurrent is larger than that of the cathodic photocurrent, while at bentonite clay-coated electrodes the

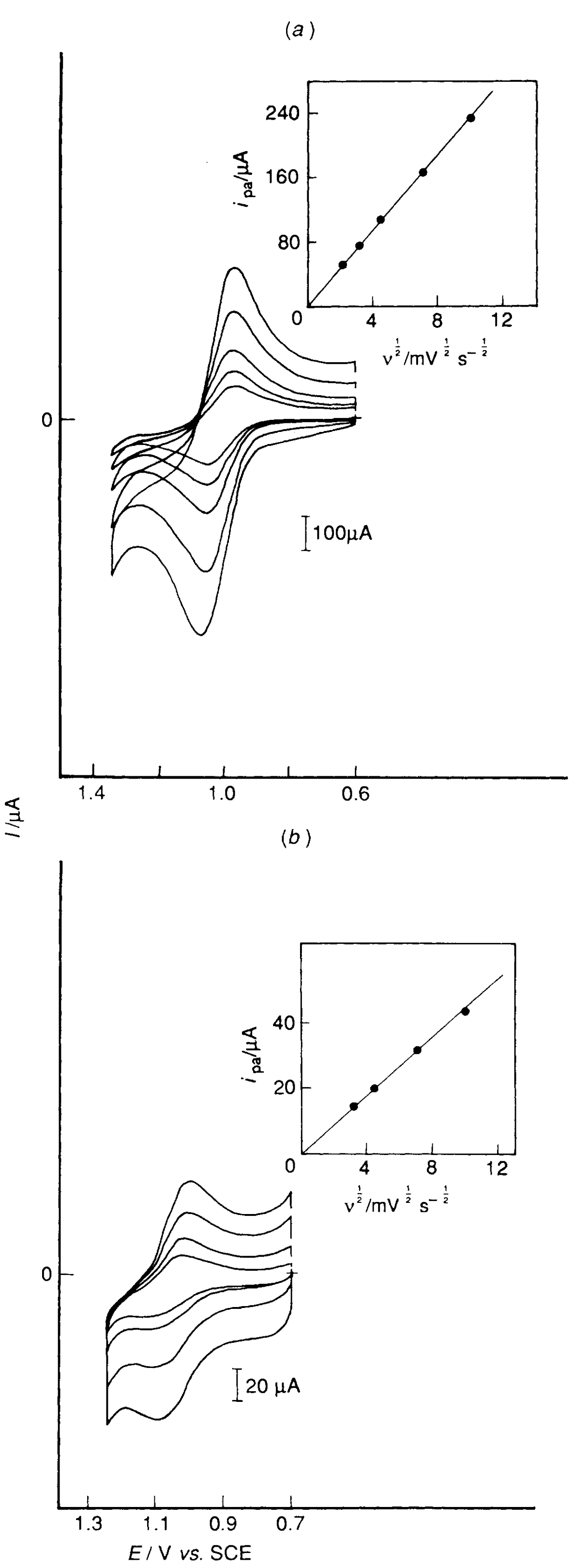

Fig. 1 Cyclic voltammograms of the $[Ru(bipy)_3]^{2+/3+}$ couple at Pt–nf–$[Ru(bipy)_3]^{2+}$ (*a*) and Pt–H^+-bt–$[Ru(bipy)_3]^{2+}$ (*b*) electrodes in an aqueous solution containing 0.1 mol dm^{-3} $HClO_4$. Scan rate = 5, 10, 20, 50 and 100 (*a*) and 10, 20, 50 and 100 mV s^{-1} (*b*). Inset: dependence of peak current on the square root of the scan rate

Table 1 Photocurrents (μA) induced at Pt–nf–$[Ru(bipy)_3]^{2+}$ and Pt–H^+-bt–$[Ru(bipy)_3]^{2+}$ electrodes with different quenchers; [quencher] = 0.15 mmol dm^{-3}, $[HClO_4]$ = 0.1 mol dm^{-3}

	Pt–nf–$[Ru(bipy)_3]^{2+}$		Pt–H^+-bt–$[Ru(bipy)_3]^{2+}$	
Quencher	0[a]	1.3 V[b]	0[a]	1.3 V[b]
$[Co(cyclam)(H_2O)_2]^{3+}$	17	−55	24	−7
$[Co(hmtd)(H_2O)_2]^{3+}$	19	−40	13	−5
$[Co(hmtd)(H_2O)(NO_2)]^{2+}$	30	−58	8	−3
Fe^{3+}	15	−50	39	−8

[a] Cathodic photocurrents induced at an applied potential of 0 V *vs.* SCE. [b] Anodic photocurrents induced at an applied potential of 1.3 V *vs.* SCE.

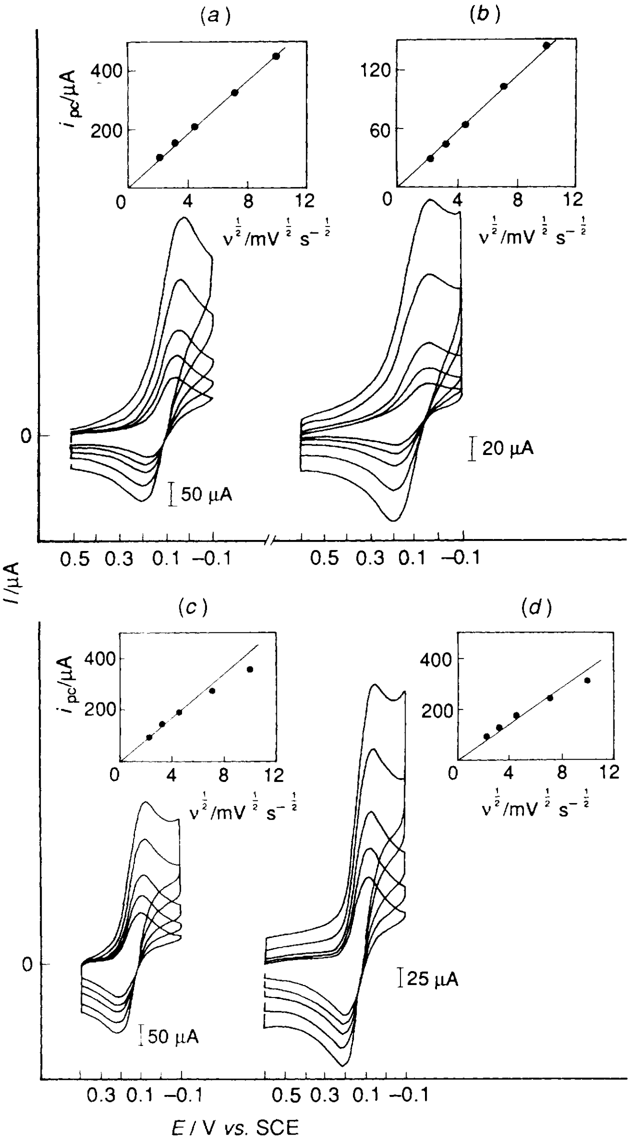

Fig. 2 Cyclic voltammograms of 0.15 mmol dm^{-3} [Co(cyclam)-$(H_2O)_2]^{3+/2+}$ at Pt–nf (*a*), Pt–nf–$[Ru(bipy)_3]^{2+}$ (*b*), Pt–H^+-bt (*c*) and Pt–H^+-bt–$[Ru(bipy)_3]^{2+}$ (*d*) electrodes in an aqueous solution containing 0.1 mol dm^{-3} $HClO_4$. Scan rate = 5, 10, 20, 50 and 100 mV s^{-1}. Inset: dependence of peak current on the square root of the scan rate

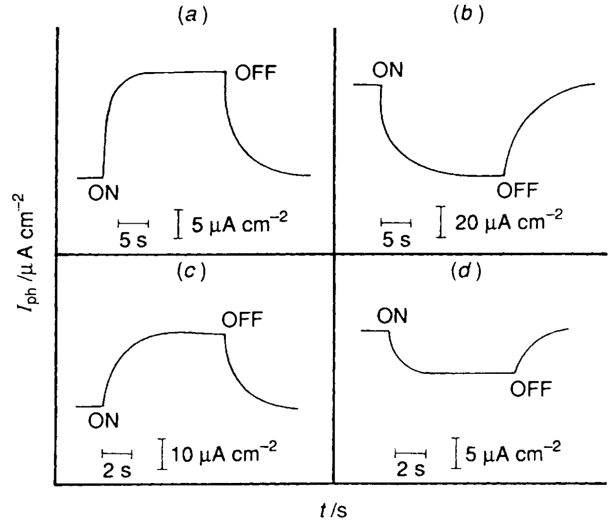

Fig. 3 Photocurrent responses to switching 'on' and 'off' of irradiation at the Pt–nf–$[Ru(bipy)_3]^{2+}$ (*a*, *b*) and Pt–H^+-bt–$[Ru(bipy)_3]^{2+}$ (*c*, *d*) electrodes in a solution containing 0.15 mmol dm^{-3} [Co(cyclam)-$(H_2O)_2]^{3+}$ and 0.1 mol dm^{-3} $HClO_4$ and at applied potentials of 0 (*a*, *c*) and 1.3 V *vs.* SCE (*b*, *d*)

magnitude of the cathodic photocurrent is larger than that of the anodic photocurrent. It has already been established[41–44] that the Nafion film favours the oxidation process by favouring the formation of the more positively charged metal complex, and the clay film favours the reduction process by favouring the formation of the less positively charged metal complex. In the present investigation the electrochemical data obtained using the coated electrodes are also in line with those for the reported systems.[41–44]

The photoelectrochemical behaviour observed with different coated electrodes clearly suggests that the photoproduced species, $[Ru(bipy)_3]^{3+}$ and $[Co(cyclam)(H_2O)_2]^{2+}$, are participating in the electron-transfer reactions at the coated electrode. During irradiation, $[Ru(bipy)_3]^{2+}$ adsorbed into the film absorbs light and the resulting excited state $*[Ru(bipy)_3]^{2+}$ reacts with $[Co(cyclam)(H_2O)_2]^{3+}$ oxidatively to produce $[Ru(bipy)_3]^{3+}$ and $[Co(cyclam)(H_2O)_2]^{2+}$. The electrode reactions of the photoproduced $[Ru(bipy)_3]^{3+}$ and $[Co(cyclam)(H_2O)_2]^{2+}$ are responsible for the cathodic and anodic photocurrents at different applied potentials and can be summarized as in Scheme 1.

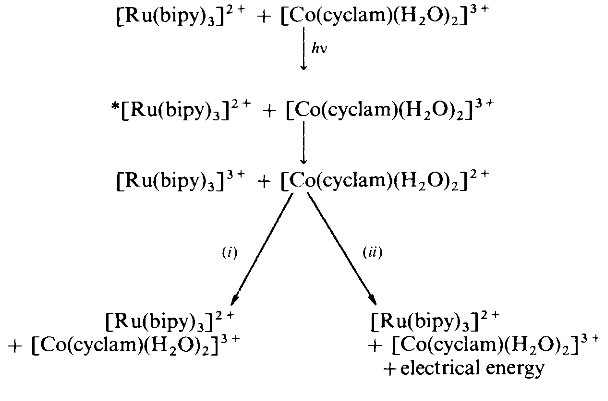

Scheme 1 (*i*) Back electron transfer; (*ii*) electrodic reactions

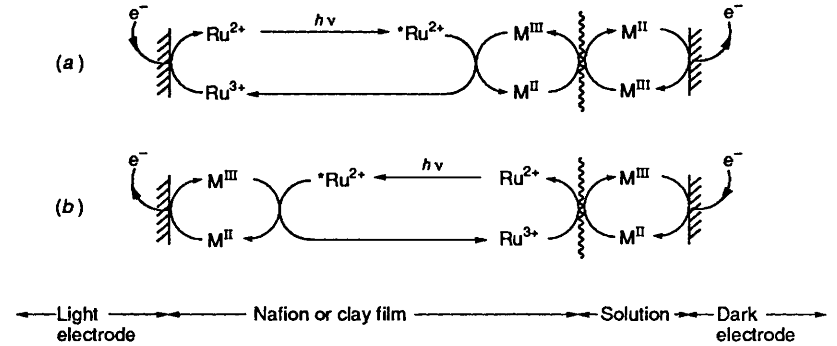

Scheme 2 Reactions at Pt–nf–$[Ru(bipy)_3]^{2+}$ and Pt–bt–$[Ru(bipy)_3]^{2+}$ electrodes under applied potentials of 0 (*a*) and 1.3 V (*b*) *vs.* SCE. Ru^{2+} represents $[Ru(bipy)_3]^{2+}$ and M^{III} represents Fe^{3+}, $[Co(cyclam)(H_2O)_2]^{3+}$, $[Co(hmtd)(H_2O)_2]^{3+}$ or $[Co(hmtd)(H_2O)(NO_2)]^{2+}$

At 0 V *vs.* SCE the cathodic photocurrent indicates that the photoproduced $[Ru(bipy)_3]^{3+}$ species undergo reduction to produce $[Ru(bipy)_3]^{2+}$ at light-irradiated Pt–nf–$[Ru(bipy)_3]^{2+}$ or Pt–bt–$[Ru(bipy)_3]^{2+}$ electrodes, following the quenching reaction of $*[Ru(bipy)_3]^{2+}$ with $[Co(cyclam)(H_2O)_2]^{3+}$ (Fig. 3). When a photoelectrochemical cell was constructed with either of these two electrodes and dipped in a mixture containing $[Co(cyclam)(H_2O)_2]^{3+}$ and H^+ ion the coated electrode would act as photocathode and the plain platinum counter electrode as anode at which the photoproduced $[Co(cyclam)(H_2O)_2]^{2+}$ ion undergoes oxidation [equation (1)].

$$[Ru(bipy)_3]^{3+} + e^- \longrightarrow [Ru(bipy)_3]^{2+} \qquad (1)$$

At 1.3 V *vs.* SCE the anodic photocurrent results from the oxidation of photoproduced $[Co(cyclam)(H_2O)_2]^{2+}$ at light-irradiated Pt–nf–$[Ru(bipy)_3]^{2+}$ or Pt–bt–$[Ru(bipy)_3]^{2+}$ electrode, following the quenching reaction of $*[Ru(bipy)_3]^{2+}$ with $[Co(cyclam)(H_2O)_2]^{3+}$ (Fig. 3). In a cell containing either of these electrodes dipped in $[Co(cyclam)(H_2O)_2]^{3+}$ and H^+ ion the coated electrode would act as photoanode and the plain platinum counter electrode as cathode at which $[Co(cyclam)(H_2O)_2]^{3+}$ undergoes reduction [equation (2)]. The different

$$[Co(cyclam)(H_2O)_2]^{2+} \longrightarrow [Co(cyclam)(H_2O)_2]^{3+} + e^- \qquad (2)$$

electrodic reactions responsible for the anodic and cathodic photocurrent generation at different applied potentials are summarized in Scheme 2.

The cyclic voltammograms recorded for Pt–nf–$[Ru(bipy)_3]^{2+}$ and Pt–H^+-bt–$[Ru(bipy)_3]^{2+}$ electrodes dipped in a solution containing 1 mmol dm^{-3} Fe^{3+} ion and 0.1 mol dm^{-3} $HClO_4$ with and without visible light illumination are shown in Fig. 4. The time profiles of the photocurrents were recorded for the two electrodes dipped in 0.15 mmol dm^{-3} Fe^{3+} ion and 0.1 mol dm^{-3} $HClO_4$ at various applied potentials with light-on and -off conditions and are shown in Fig. 5(*a*) and 5(*b*). The cathodic photocurrent observed at an applied potential of 0 V *vs.* SCE gradually decreases at more positive potentials and the onset of an anodic photocurrent was observed around 0.8 V *vs.* SCE. Similarly, the photocurrents were measured at different applied potentials using the same electrodes in an aqueous solution of 0.15 mmol dm^{-3} $[Co(cyclam)(H_2O)_2]^{3+}$ and 0.1 mol dm^{-3} $HClO_4$ and are shown in Fig. 6(*a*) and 6(*b*).

Scheme 2 is further supported by the photoresponses observed with Pt–nf–$[Ru(bipy)_3]^{2+}$ and Pt–bt–$[Ru(bipy)_3]^{2+}$ electrodes in an aqueous solution containing 0.15 mmol dm^{-3} $[Co(cyclam)(H_2O)_2]^{3+}$, 0.1 mol dm^{-3} $HClO_4$ and O_2 or triethanolamine. Both electrodes at an applied potential of 0 V *vs.* SCE showed a greatly enhanced cathodic photocurrent in O_2-saturated solution, while there is no obvious change in the anodic photocurrent observed at 1.3 V *vs.* SCE. At the Pt–nf–$[Ru(bipy)_3]^{2+}$ electrode at an applied potential of 0 V *vs.* SCE a cathodic photocurrent of 190 μA cm^{-2} was observed for an air-saturated solution under the above conditions, which is *ca.* 11 times higher than that observed in the absence of O_2 (Table 1). This surely arises due to the oxidation of photoproduced $[Co(cyclam)(H_2O)_2]^{2+}$ species by O_2,[34] which would retard the back electron transfer between $[Ru(bipy)_3]^{3+}$ and $[Co(cyclam)(H_2O)_2]^{2+}$ resulting in the increase in $[Ru(bipy)_3]^{3+}$ concentration and hence the cathodic photocurrent.

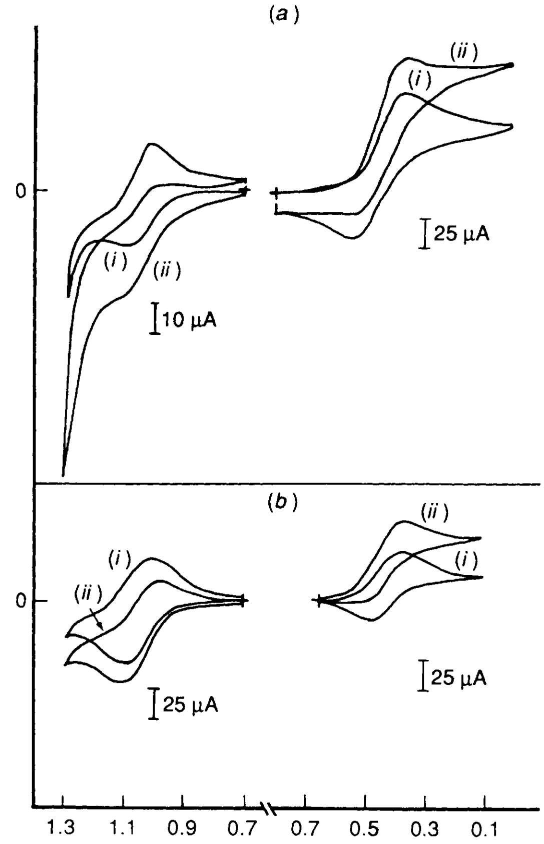

Fig. 4 Cyclic voltammograms of Pt–H^+-bt–$[Ru(bipy)_3]^{2+}$ (*a*) and Pt–nf–$[Ru(bipy)_3]^{2+}$ (*b*) electrodes, without (*i*) and with illumination (*ii*), in a solution containing 1×10^{-3} mol dm^{-3} Fe^{3+} ion and 0.1 mol dm^{-3} $HClO_4$; scan rate = 2 mV s^{-1}

Under an applied potential of 1.3 V *vs.* SCE a greatly enhanced anodic photocurrent was observed at both Pt–nf–$[Ru(bipy)_3]^{2+}$ and Pt–bt–$[Ru(bipy)_3]^{2+}$ electrodes when dipped in a solution of 0.15 mmol dm^{-3} $[Co(cyclam)(H_2O)_2]^{3+}$, 0.1 mol dm^{-3} $HClO_4$ and 0.1 mol dm^{-3} triethanolamine, while there is no obvious change in the cathodic photocurrent observed at 0 V *vs.* SCE. At the former electrode and an applied

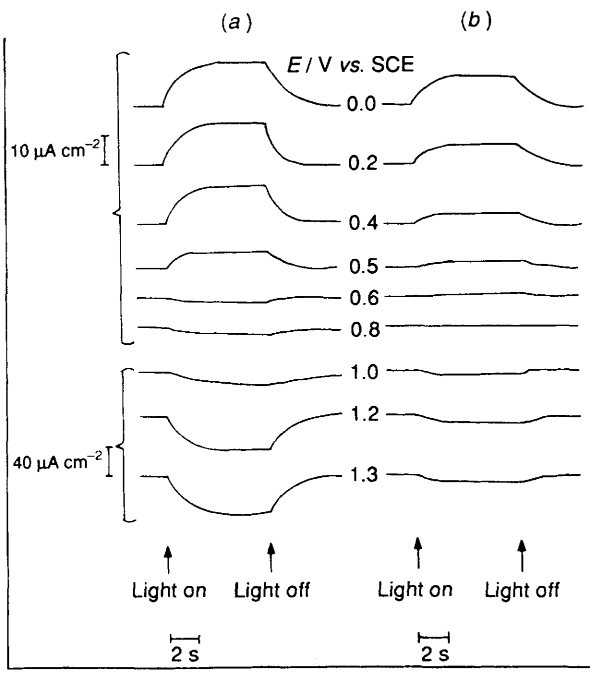

Fig. 5 Photocurrent *vs.* time responses of Pt–nf–[Ru(bipy)$_3$]$^{2+}$ (*a*) and Pt–H$^+$-bt–[Ru(bipy)$_3$]$^{2+}$ (*b*) electrodes held at different potentials and dipped in a solution of 0.15 mmol dm^{-3} Fe^{3+} ion and 0.1 mol dm^{-3} HClO$_4$

potential of 1.3 V *vs.* SCE an anodic photocurrent of 175 µA cm^{-2} was observed under these conditions which is *ca.* 25 times greater than that observed in the absence of triethanolamine (Table 1). The enhanced anodic photocurrent results from the reduction of photochemically produced [Ru(bipy)$_3$]$^{3+}$ by triethanolamine and corresponding build-up of [Co(cyclam)(H$_2$O)$_2$]$^{2+}$. This facile reduction of [Ru(bipy)$_3$]$^{3+}$ retards the back electron transfer between [Ru(bipy)$_3$]$^{3+}$ and [Co(cyclam)(H$_2$O)$_2$]$^{2+}$, resulting in the increase in [Co(cyclam)(H$_2$O)$_2$]$^{2+}$ concentration and hence the anodic photocurrent.

The rate constant, k_q, for the quenching of *[Ru(bipy)$_3$]$^{2+}$ can be calculated photoelectrochemically using photocurrents induced at Pt–nf–[Ru(bipy)$_3$]$^{2+}$ and Pt–bt–[Ru(bipy)$_3$]$^{2+}$ electrodes under different quencher concentrations. The dependence of the photocurrent (I_{ph}) on the quencher concentration [Q] is given by relation (3)[46] where F is the Faraday constant,

$$\frac{1}{I_{ph}} = \frac{k^{\frac{1}{2}}}{2FA\alpha I_0 c_0 D^{\frac{1}{2}}}\left[1 + \frac{k_0}{k_q[Q]}\right] \qquad (3)$$

A is the surface area of the coated electrode, α is the absorption coefficient of [Ru(bipy)$_3$]$^{2+}$, I_0 is the intensity of light incident on the coated electrode, c_0 is the initial concentration of [Ru(bipy)$_3$]$^{2+}$, D is the diffusion coefficient of [Ru(bipy)$_3$]$^{2+}$, k_0 is the phosphorescence decay constant for the excited state *[Ru(bipy)$_3$]$^{2+}$, and k is the pseudo-first-order rate constant for the reduction of [Ru(bipy)$_3$]$^{3+}$ by water molecules [equation (7)]. It has been reported that the reduction of photochemically produced [Ru(bipy)$_3$]$^{3+}$ by water molecules occurs in addition to other reaction pathways and this reduction process is also dependent on pH.[47] Equation (3) indicates that a plot of I_{ph}^{-1} *vs.* [Q]$^{-1}$ should be linear with a slope $k_0 k^{\frac{1}{2}}/2FA\alpha I_0 c_0 k_q D^{\frac{1}{2}}$ and intercept $k^{\frac{1}{2}}/2FA\alpha I_0 c_0 D^{\frac{1}{2}}$. Scheme 3 is proposed to explain the excited state *[Ru(bipy)$_3$]$^{2+}$ quenching at the modified electrodes.

The quenching rate constants at Pt–nf–[Ru(bipy)$_3$]$^{2+}$ and Pt–bt–[Ru(bipy)$_3$]$^{2+}$ electrodes can be calculated for the quenching reaction between *[Ru(bipy)$_3$]$^{2+}$ and Fe^{3+}/

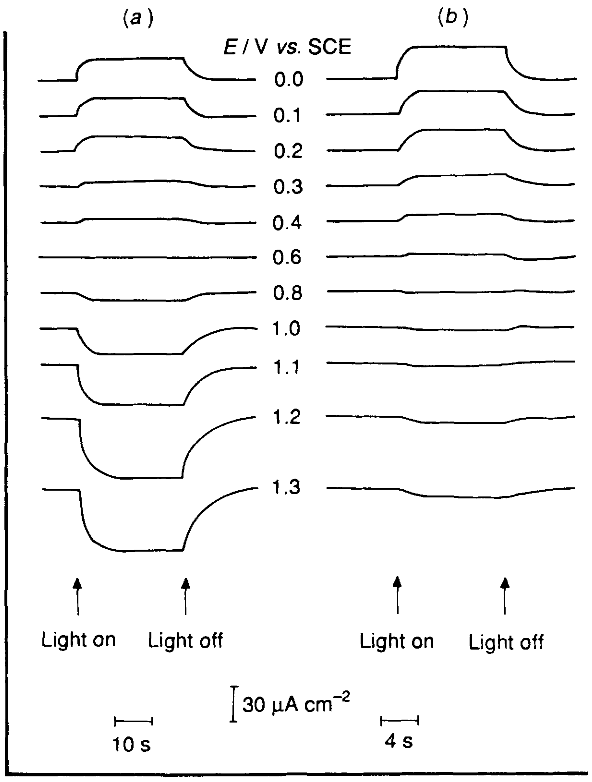

Fig. 6 Photocurrent *vs.* time responses of the electrodes in Fig. 5 dipped in a solution of 0.15 mmol dm^{-3} [Co(cyclam)(H$_2$O)$_2$]$^{3+}$ and 0.1 mol dm^{-3} HClO$_4$

$$[\text{Ru(bipy)}_3]^{2+} \xrightarrow{h\nu} {}^*[\text{Ru(bipy)}_3]^{2+} \qquad (4)$$

$$ {}^*[\text{Ru(bipy)}_3]^{2+} \xrightarrow{k_0} \begin{cases} [\text{Ru(bipy)}_3]^{2+} + \text{light} \\ [\text{Ru(bipy)}_3]^{2+} + \text{heat} \end{cases} \qquad (5)$$

$$ {}^*[\text{Ru(bipy)}_3]^{2+} + \text{M}^{3+} \xrightarrow{k_q} [\text{Ru(bipy)}_3]^{3+} + \text{M}^{2+} \qquad (6)$$

$$[\text{Ru(bipy)}_3]^{3+} + e^- \longrightarrow [\text{Ru(bipy)}_3]^{2+} \ \text{(at coated electrode)} \qquad (1)$$

$$2[\text{Ru(bipy)}_3]^{3+} + \text{H}_2\text{O} \xrightarrow{k} 2[\text{Ru(bipy)}_3]^{2+} + \tfrac{1}{2}\text{O}_2 + 2\text{H}^+ \qquad (7)$$

Scheme 3 M^{3+} represents Fe^{3+} or cobalt(III) complex

cobalt(III) complexes using equation (8), considering the fact

$$\frac{1}{I_{ph}} = \text{intercept}\left[1 + \frac{k_0}{k_q[Q]}\right] \qquad (8)$$

that the diffusion-controlled electron-transfer process occurs in homogeneous solution as well as in Nafion- and clay-coated systems.

For both Pt–nf–[Ru(bipy)$_3$]$^{2+}$ and Pt–Na$^+$-bt–[Ru(bipy)$_3$]$^{2+}$ electrodes, the cathodic photocurrents were measured at 0 V *vs.* SCE at different concentrations of [Co(cyclam)(H$_2$O)$_2$]$^{3+}$. A plot of I_{ph}^{-1} *vs.* [Co(cyclam)(H$_2$O)$_2{}^{3+}$]$^{-1}$ gave a straight line with an intercept as shown in Fig. 7. At the former electrode the quenching rate constant, k_q, has been evaluated to be 2.6 × 10^{10} dm^3 mol^{-1} s^{-1} from the values of the slope and intercept, using a k_0 value of 1.6 × 10^6 s^{-1} for [Ru(bipy)$_3$]$^{2+}$ adsorbed into Nafion film.[48] At the latter electrode, k_q has been calculated to be 4.0 × 10^{10} dm^3 mol^{-1} s^{-1}. In the case of clay-adsorbed [Ru(bipy)$_3$]$^{2+}$, a value of 2.4 × 10^6 s^{-1} for k_0 was used.[49] The reported excited-state lifetimes of [Ru(bipy)$_3$]$^{2+}$ adsorbed into Nafion film and clay colloid are used for the

Table 2 Quenching rate constants obtained at Pt–nf–$[Ru(bipy)_3]^{2+}$ and Pt–Na^+-bt–$[Ru(bipy)_3]^{2+}$ electrodes with different quenchers; $[HClO_4]$ = 0.1 mol dm^{-3}

	k_q/dm³ mol⁻¹ s⁻¹	
Quencher	Pt–nf–$[Ru(bipy)_3]^{2+}$	Pt–Na^+-bt–$[Ru(bipy)_3]^{2+}$
$[Co(cyclam)(H_2O)_2]^{3+}$	2.6×10^{10}	4.0×10^{10}
$[Co(hmtd)(H_2O)_2]^{3+}$	2.1×10^{10}	1.6×10^{10}
$[Co(hmtd)(H_2O)(NO_2)]^{2+}$	9.6×10^{10}	4.7×10^{10}
Fe^{3+}	2.3×10^{9}	3.7×10^{9}

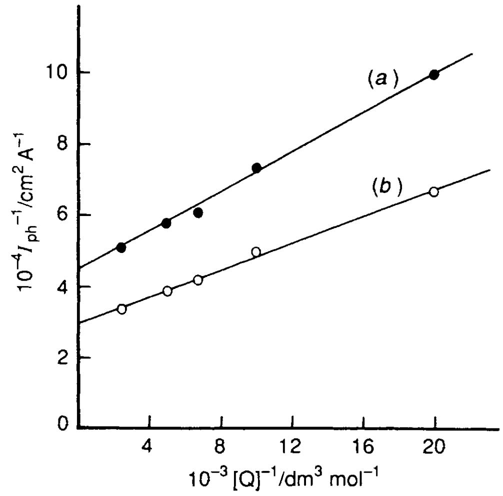

Fig. 7 Plots of the reciprocal photocurrent against the concentration of $[Co(cyclam)(H_2O)_2]^{3+}$ for Pt–nf–$[Ru(bipy)_3]^{2+}$ (*a*) and Pt–Na^+-bt–$[Ru(bipy)_3]^{2+}$ (*b*) electrodes under an applied potential of 0 V *vs.* SCE; conditions as in Fig. 3

calculation of k_q with the assumption that the present systems will be similar to the reported one.[48,49] In a similar way the k_q values were also determined for other cobalt(III) complexes and Fe^{3+} ion, and are given in Table 2.

An electrode coated with Nafion (1 μm) containing 2.49×10^{-8} mol cm⁻² $[Ru(bipy)_3]^{2+}$ when dipped in 0.025 mmol dm⁻³ Fe^{3+} ion and 0.1 mol dm⁻³ $HClO_4$ produced stable photocurrents for more than 1 h at both 0 and 1.3 V *vs.* SCE. Under irradiation the charges passed for the photochemical processes at 0 and 1.3 V *vs.* SCE in 1 h were 65×10^{-3} and 98.5×10^{-3} C, respectively. Based on these values, the turnover number for $[Ru(bipy)_3]^{2+}$ during the photoelectrochemical event was calculated to be 27 for the cathodic photocurrent observed at 0 V and 41 for the anodic photocurrent observed at 1.3 V *vs.* SCE.[12]

In conclusion, the anodic and cathodic photocurrents produced at Nafion- and clay-coated electrodes are due to the different electron-transfer reactions occurring at the coated electrodes followed by the quenching reaction. The quenching rate constants have been determined for the photoredox systems at the chemically modified electrodes using a photoelectrochemical cell.

Acknowledgements

Financial support from the Department of Science & Technology and Department of Atomic Energy, Government of India is gratefully acknowledged. K. V. G. thanks the Council of Scientific & Industrial Research for support in the form of a Senior Research Fellowship.

References

1 A. K. Edwards and D. P. Rillema, *J. Electroanal. Chem., Interfacial Electrochem.*, 1991, **314**, 165.
2 D. Rong, Y. I. Kim and T. E. Mallouk, *Inorg. Chem.*, 1990, **29**, 1531.
3 E. Barendrecht, *J. Appl. Electrochem.*, 1990, **20**, 175.
4 J. Yano, A. Shimoyama and K. Ogura, *J. Electrochem. Soc.*, 1992, **139**, L52.
5 P. Joo, *Colloids and Surfaces*, 1990, **49**, 29.
6 M. Kaneko and D. Wöhrle, *Adv. Polym. Sci.*, 1988, **84**, 141.
7 D. P. Rillema, A. K. Edwards, S. C. Perine and A. L. Crumbliss, *Inorg. Chem.*, 1991, **30**, 4421.
8 R. Ramaraj and P. Natarajan, *J. Chem. Soc., Faraday Trans. 1*, 1989, 813.
9 M. Krishnan, X. Zhang and A. J. Bard, *J. Am. Chem. Soc.*, 1984, **106**, 7371.
10 N. Oyama, S. Yamaguchi, M. Kaneko and A. Yamada, *J. Electroanal. Chem., Interfacial Electrochem.*, 1982, **139**, 215.
11 M. Kaneko, S. Hara and A. Yamada, *J. Electroanal. Chem., Interfacial Electrochem.*, 1985, **194**, 165.
12 M. Kaneko and A. Yamada, *Electrochim. Acta*, 1986, **31**, 273.
13 S. Cosnier, A. Deronzier and J.-C. Moutet, *J. Phys. Chem.*, 1985, **89**, 4895.
14 I. Willner, R. Maidan, D. Mandler, H. Dûrr, G. Dörr and K. Zengerle, *J. Am. Chem. Soc.*, 1987, **109**, 6080.
15 S. Nishida, Y. Harima and K. Yamashita, *J. Chem. Soc., Dalton Trans.*, 1991, 3401.
16 D. Kotkar, V. Joshi and P. K. Ghosh, *J. Chem. Soc., Chem. Commun.*, 1987, 4.
17 H. Nijs, J. J. Fripiat and H. Van Damme, *J. Phys. Chem.*, 1983, **87**, 1279.
18 K. V. Gobi and R. Ramaraj, *J. Electroanal. Chem., Interfacial Electrochem.*, 1994, **368**, 77.
19 T. D. Westmoreland, J. M. Calvert, R. W. Murray and T. J. Meyer, *J. Chem. Soc., Chem. Commun.*, 1983, 65.
20 Z. Porat, Y. M. Tricot, I. Rubinstein and B. Zinger, *J. Electroanal. Chem., Interfacial Electrochem.*, 1991, **315**, 217.
21 T. Okajima, T. Ohsaka and N. Oyama, *J. Electroanal. Chem., Interfacial Electrochem.*, 1991, **315**, 175.
22 D. Ege, P. K. Ghosh, J. R. White, J. F. Equey and A. J. Bard, *J. Am. Chem. Soc.*, 1985, **107**, 5644.
23 W. Grot, *Chem. Ind. (London)*, 1985, 647.
24 T. D. Gierke, presented at the Electrochemical Society Meeting, Atlanta, GA, October 9-14th, 1977, paper 438.
25 H. L. Yeager and A. Steck, *J. Electrochem. Soc.*, 1981, **128**, 1880.
26 T. D. Gierke and W. Y. Hsu, *ACS Symp. Ser.*, 1982, **180**.
27 K. A. Mauritz and A. J. Hopfinger, *Modern Aspects of Electrochemistry*, eds. J. O'M. Bockris, B. E. Conway and R. E. White, Plenum, New York, 1982, vol. 14.
28 A. C. D. Newman (Editor), *Chemistry of Clays and Clay Minerals*, Minerology Society Monograph No. 6, Wiley-Interscience, London, 1987.
29 J. M. Adams and A. Foucaud, in *Preparative Chemistry using Supported Reagents*, ed. P. Laszlo, Academic Press, London, 1987.
30 P. Laszlo, *Science*, 1987, **235**, 1473.
31 J. K. Thomas, *Acc. Chem. Res.*, 1988, **21**, 275.
32 M. Kaneko, *J. Macromol. Sci., Chem.*, 1984, **24**, 357.
33 G. Sprintschnik, H. W. Sprintschnik and D. G. Whitten, *J. Am. Chem. Soc.*, 1976, **98**, 2337.
34 T. Geiger and F. C. Anson, *J. Am. Chem. Soc.*, 1981, **103**, 7489.
35 B. Bosnich, C. K. Poon and M. L. Tobe, *Inorg. Chem.*, 1965, **4**, 1102.
36 N. Sadasivan, J. A. Kernohan and J. F. Endicott, *Inorg. Chem.*, 1967, **6**, 770.
37 P. O. Whimp and N. F. Curtis, *J. Chem. Soc. A*, 1966, 867.
38 C. M. Castro-acuna, F. F. Fan and A. J. Bard, *J. Electroanal. Chem., Interfacial Electrochem.*, 1987, **234**, 347.
39 A. J. Bard and O. Enea, *J. Phys. Chem.*, 1986, **90**, 301.
40 R. E. Grim, *Clay Minerology*, McGraw-Hill, New York, 1953.

41 H. Y. Liu and F. C. Anson, *J. Electroanal. Chem., Interfacial Electrochem.*, 1985, **184**, 411.

42 C. M. Lieber, M. H. Schmidt and N. S. Lewis, *J. Phys. Chem.*, 1986, **90**, 1002.

43 R. Naegeli, J. Redepenning and F. C. Anson, *J. Phys. Chem.*, 1986, **90**, 6227.

44 M. E. Gomez and A. E. Kaifer, *J. Chem. Educ.*, 1992, **69**, 502.

45 I. Rubinstein and A. J. Bard, *J. Am. Chem. Soc.*, 1981, **103**, 5007.

46 S. Nishida, Y. Harima and K. Yamashita, *Inorg. Chem.*, 1989, **28**, 4073.

47 R. Memming and F. Schröppel, *Chem. Phys. Lett.*, 1979, **62**, 207.

48 R. Lin, T. Onikubo, K. Nagai and M. Kaneko, *J. Electroanal. Chem., Interfacial Electrochem.*, 1993, **348**, 189.

49 R. A. DellaGuardia and J. K. Thomas, *J. Phys. Chem.*, 1983, **87**, 990.

Received 28*th April* 1994; *Paper* 4/02529F